

RESEARCH

Open Access



Upregulation of dihydropyrimidinase-like 3 (DPYSL3) protein predicts poor prognosis in urothelial carcinoma

Peir-In Liang¹, Hong-Yue Lai², Ti-Chun Chan^{2,3}, Wei-Ming Li^{4,5,6,7}, Chung-Hsi Hsing^{2,8}, Steven K. Huang^{9,10}, Kun-Lin Hsieh⁹, Wen-Hsin Tseng⁹, Tzu-Ju Chen^{11,12}, Wan-Shan Li^{12,13}, Huan-Da Chen¹, Yu-Hsuan Kuo^{14,15*} and Chien-Feng Li^{2,3*}

Abstract

Background Dihydropyrimidinase-like 3 (DPYSL3) is a cytosolic phosphoprotein expressed in the nervous system and is crucial for neurogenesis. A previous study showed that increased DPYSL3 expression promotes tumour aggressiveness in pancreatic ductal adenocarcinoma, gastric cancer, and colon cancer. However, the role of DPYSL3 in affecting the biological behaviour of urothelial carcinoma (UC) is not yet understood.

Methods A UC transcriptomic dataset from the Gene Expression Omnibus and the Urothelial Bladder Cancer (BLCA) dataset from The Cancer Genome Atlas were used for the in silico study. We collected 340 upper urinary tract urothelial carcinoma (UTUC) and 295 urinary bladder urothelial carcinoma (UBUC) samples for the immunohistochemical study. Fresh tumour tissue from 50 patients was used to examine the DPYSL3 mRNA level. In addition, urothelial cell lines with and without *DPYSL3* knockdown were used for the functional study.

Results The in silico study revealed that DPYSL3 correlated with advanced tumour stage and metastasis development while functioning primarily in the nucleobase-containing compound metabolic process (GO:0006139). *DPYSL3* mRNA expression is significantly upregulated in advanced UC. Furthermore, overexpression of the DPYSL3 protein is significantly associated with the aggressive behaviour of UTUC and UBUC. DPYSL3 expression independently predicts disease-specific survival (DSS) and metastatic-free survival (MFS) in patients with UC. In non-muscle-invasive UBUC, DPYSL3 expression predicts local recurrence-free survival. UC cell lines with *DPYSL3* knockdown exhibited decreased proliferation, migration, invasion, and human umbilical vein endothelial cells (HUVECs) tube formation but increased apoptosis and G1 arrest. Gene ontology enrichment analysis revealed that the enriched processes related to DPYSL3 overexpression in UC were tissue morphogenesis, cell mesenchyme migration, smooth muscle regulation, metabolic processes, and RNA processing. In vivo study revealed *DPYSL3* knockdown in UC tumours significantly suppressed the growth of tumours and decreased MYC and GLUT1 protein expression.

Conclusions DPYSL3 promotes the aggressiveness of UC cells by changing their biological behaviours and is likely associated with cytoskeletal and metabolic process modifications. Furthermore, DPYSL3 protein overexpression in UC

*Correspondence:

Yu-Hsuan Kuo
a10901@mail.chimei.org.tw
Chien-Feng Li
angelo.p@yahoo.com.tw

Full list of author information is available at the end of the article



© The Author(s) 2023. **Open Access** This article is licensed under a Creative Commons Attribution 4.0 International License, which permits use, sharing, adaptation, distribution and reproduction in any medium or format, as long as you give appropriate credit to the original author(s) and the source, provide a link to the Creative Commons licence, and indicate if changes were made. The images or other third party material in this article are included in the article's Creative Commons licence, unless indicated otherwise in a credit line to the material. If material is not included in the article's Creative Commons licence and your intended use is not permitted by statutory regulation or exceeds the permitted use, you will need to obtain permission directly from the copyright holder. To view a copy of this licence, visit <http://creativecommons.org/licenses/by/4.0/>. The Creative Commons Public Domain Dedication waiver (<http://creativecommons.org/publicdomain/zero/1.0/>) applies to the data made available in this article, unless otherwise stated in a credit line to the data.

was associated with aggressive clinicopathological characteristics and independently predicted poor clinical outcomes. Therefore, DPYSL3 can be used as a novel therapeutic target for UC.

Keywords Dihydropyrimidinase-like 3 (DPYSL3), Upper urinary tracts urothelial carcinoma (UTUC), Urinary bladder urothelial carcinoma (UBUC), Cytoskeleton modification, Mammalian target of rapamycin (mTOR), Ribosomal protein S6 (RPS6), Cellular Myelocytomatosis (C-Myc), Glucose transporter 1 (GLUT1), Metabolic process reprogramming

Background

Urothelial carcinoma (UC) is a common tumour that involves the upper urinary tract (renal pelvis and ureter, UTUC) or urinary bladder (UBUC). UTUC is less frequently seen than UBUC, accounting for 5%~10% of all UC cases worldwide. However, a higher incidence of UTUC is seen in populations associated with Balkan endemic nephropathy, Chinese herb nephropathy, and phenacetin abuse [1–3]. The prevalence of UTUC in Taiwan has progressively increased in recent years, accounting for more than 40% of UC cases. Exposure to aristolochic acid-containing herbal medicines plays a vital role in the high incidence of UTUC in Taiwan [4].

UC has heterogeneous biological behaviours with a wide range of recurrence and progression probabilities. Most patients (~75%) with newly diagnosed UBUC have non-muscle invasive bladder cancer (NMIBC). The five-year tumour-specific survival rates for early and advanced UBUC are >90% and ~60%, respectively [5]. In contrast, UTUC patients have a more dismal outcome. Most UTUC patients have advanced tumour stage (>pT2) at the initial diagnosis [6, 7]. The 5-year disease-specific survival rate of patients with advanced disease is less than 50% [8]. Whether UBUC and UTUC harbour the same molecular alterations is controversial. However, some studies have shown that the gene expression profile and the frequently mutated genes of UTUC and UBUC showed some similarities [2, 9]. These findings indicated that some aspects of UBUC and UTUC tumorigenesis might have common pathways. A comprehensive understanding of UC biology is essential for developing new treatment modalities.

Rapid growth and proliferation are characteristics of cancer cells, and require the facilitation of DNA and RNA biosynthesis in tumour cells. Therefore, cancer cells reprogram the nucleotide production and degradation processes to preserve the nucleotide pools to achieve this requirement. Interfering with nucleotide metabolism is a frequently used strategy in cancer treatment [10]. Using the transcriptomic dataset GSE31684 from the Gene Expression Omnibus (GEO) and focusing on the nucleobase-containing compound metabolic process (GO:0006139), we identified DPYSL3 as the gene that is significantly correlated with UBUC patients prognosis.

Dihydropyrimidinase-like 3 (DPYSL3), also called collapsing response mediator protein 4 (CRMP4), is a cytosolic phosphoprotein highly expressed in the nervous system [11–14]. The protein product of the *DPYSL3* gene, located on chromosome 5q32, is crucial for many aspects of neurogenesis, including neuronal differentiation, neurite outgrowth, and axonal guidance [14–16]. Overexpression of DPYSL3 in neurons induces filopodia formation and neurite branching [17]. These phenomena are likely a result of DPYSL3-mediated modifications of the neuronal cytoskeleton, such as bundling with F-actin filaments [18]. Previous studies have shown that DPYSL3 has diverse effects on altering cancer cell aggressiveness [19–24]. Decreased DPYSL3 expression in prostate cancer cells enhances cell invasion and migration abilities [23]. Increasing DPYSL3 expression in advanced neuroblastoma improves clinical outcomes [25]. However, the opposite results were observed in pancreatic ductal carcinoma, gastric cancer, and lung cancer. An *in vivo* study showed that tumours derived from DPYSL3-silenced colon cancer cells have a lower growth rate [22]. Since DPYSL3 actively regulates cancer cell invasion and proliferation, understanding its role in promoting UC cell aggressiveness is essential.

In this study, we revealed that DPYSL3 overexpression in UC is associated with tumour aggressiveness. Knock down of DPYSL3 expression in UC cell lines decreased tumour invasiveness, suppressed angiogenesis, induced apoptosis, and altered energy metabolic processes. This study showed the molecular function of DPYSL3 in UC tumorigenesis, indicating that DPYSL3 may be used as a therapeutic target in the future.

Methods

Data mining of public databases

The GSE31684 dataset (<http://www.ncbi.nlm.nih.gov/geo/query/acc.cgi?acc=GSE31684>) from the NCBI GEO database (GEO, National Center for Biotechnology Information, Bethesda, MD, USA) was selected for transcriptome expression profile analysis. This dataset contains microarray-based expression profiles of surgical specimens from 93 UBUC patients. The investigation was performed with Nexus Expression 3 software (BioDiscovery, EI Segundo, CA, USA). The significantly differentially expressed transcripts in advanced UBUC

(pT2-pT3), compared to early-stage UBUC (pTa-pT1), were identified using supervised comparative analysis. In addition, transcripts related to the “nucleobase-containing compound metabolic process” (GO:0006139) were selected for further analysis. Finally, survival analyses of the patients with high and low transcript expression were conducted to validate the impact of the identified genes on survival.

Study population

The cohort for the immunohistochemical study consisted of 340 samples of UTUC and 295 samples of UBUC collected at ChiMei Medical Hospital between 1984 and 2004. All subjects were newly diagnosed patients who received curative surgery without prior therapy. All UBUC patients with stage pT3 or higher tumours received radical cystectomy followed by cisplatin-based adjuvant chemotherapy, regardless of the status of nodal metastasis. For UTUC, some patients ($n=29$) with pT3 or pT4 tumours received additional adjuvant therapy after surgery. The clinical data were collected retrospectively from the patient medical charts. The clinicopathological evaluation criteria were mentioned in a previous study [26]. The pathological slides of all patients were reassessed to collect the pathological data. Another cohort of 20 UBUC patients from the same institution was used for quantitative mRNA analysis. The Institutional Review Board approved this study (IRB10501-005).

Quantitative real-time PCR

Fresh tumour tissues were collected and preserved by snap freezing. We used the Veritas™ automated laser capture microdissection (LCM) system (Arcturus Engineering, USA) to isolate pure UCUB cells from the snap-frozen samples. Three 7 μ m serially sliced sections were placed onto a PEN-membrane slide and stained with a HistoGene LCM Staining Kit. Approximately 1500 UCUB cells were isolated from each fresh sample. The RNA extracted using the RNeasy Mini Kit (QIAGEN) was used for cDNA synthesis. The transcript abundance of *DPYSL3* (Hs00910737_ml) mRNA was measured with *POLR2A* (Hs01108291_ml) mRNA used as an internal control. In addition, the fold change in *DYPSL3* expression was calculated. The procedure details are documented in our previous work [27].

Immunohistochemical study

Sections of formalin-fixed paraffin-embedded tissue with a thickness of 4 μ m were prepared according to the standard procedure. The sections were incubated with antibodies (Table S1a) for an hour after antigen retrieval. We used the DAKO ChemMate Envision Kit (K5001; Agilent, USA) to detect the primary antibodies.

A tumour cell was considered to exhibit positive staining when the brown signal was found in the cellular compartment corresponding to the localization of the target proteins. For surgical specimens, three 1 mm tissue cores from representative tumour areas were removed from the formalin-fixed paraffin-embedded (FFPE) blocks of each patient and used to construct recipient blocks of tissue microarrays (TMAs).

Two pathologists (PIL & CFL) blinded to the clinical data individually evaluated the stained slides to interpret and score the immunoreactivity of *DPYSL3*. The percentages of tumour cells expressing different levels of chromogen intensity were obtained. The H-score was calculated using the equation,

$$H - \text{score} = \sum P_i(i + 1),$$

where P_i indicates the percentage of tumour cells (0% to 100%) with a specific intensity, and i denotes the intensity (0 to 4+). This equation generates a score ranging from 100 to 500, where 100 indicates that all tumour cells were negative, and 500 indicates that 100% of the tumour cells stained strongly for *DPYSL3* [28, 29]. UBUC samples with an H-score higher than the median H-score of all UBUC samples were considered to exhibit high expression and those with a H-score lower than the median H-score of all UBUC samples were considered to exhibit low expression. A similar method was also applied to analyse UTUC samples.

Cell culture and stable *DPYSL3* knockdown clones establishment

The UC cells RT4, T24, BFTC905, and BFTC909 were obtained from the Bioresource Collection and Research Center (Hsinchu, Taiwan). UMUC3 and TCCSUP cells were acquired from the American Type Culture Collection (ATCC, Manassas, VA 20108, USA). The growth conditions and medium for each UC cell line were implemented as recommended. After screening *DPYSL3* protein levels using Western blot analysis, two cell lines, BFTC909 and T24, were selected to generate stable clones. The selected cells were infected with lentivirus carrying a short hairpin RNA sequence to knock down *DPYSL3* in UC cells. The procedure details are documented in our previous work [30]. The lentivirus was purchased from the National RNAi Core Facility, Genomic Research Center of the Institute of Molecular Biology, Academia Sinica, Taiwan, and the shRNA sequences were pLKO.1-*shLacZ* (TRCN0000072223: 5'-TGTTTCG C ATTATCCGAACCAT-3'), pLKO.1-*shDPYSL3*#1 (TRCN0000046848, 5'-CGGCATAGATGGAACCCA TTA-3'), and pLKO.1-*shDPYSL3*#2 (TRCN 0000046850, 5'-GCGGCAGAGTACAACATCTTT-3').

Western blot analysis

Total protein (25 µg) extracted from each UC cell line was separated on a 4–12% SDS–PAGE gel (NuPAGE; Invitrogen, USA) and transferred onto a polyvinylidene fluoride (PVDF) membrane (Amersham Biosciences, UK). The protein containing membrane was then blocked using 5% skim milk in Tris-buffered saline with Tween[®] 20 (TBST) at room temperature for one hour. Next, the membrane was incubated with antibodies (Table S1b) at 4 °C overnight. An anti-GAPDH antibody (6C5, 1:10,000; Millipore, USA) was used as a loading control antibody. The membranes were then incubated with secondary antibodies at room temperature for 90 min. Proteins were detected by enhanced chemiluminescence reagents (Amersham Biosciences, UK) and protein expression was semiquantitatively measured using densitometry.

Cell proliferation assay

This experiment was carried out using the Cell Proliferation Assay Kit (Fluorometric; BioVision, USA) and was performed according to the manufacturer's recommendation. In brief, approximately 1500 cells were plated on a 96-well dish and incubated at 37 °C and 5% CO₂. At the end of the incubation period (24, 48, and 72 h), 25 µl of lysis buffer and nuclear staining mixture was added. After a short incubation period, a microplate reader (GM3000; Promega Corp, USA) was used to measure the fluorescence intensity with the excitation/emission wavelengths set at 480/538 nm. *The procedure details* are documented in our previous work [30].

Cell migration and invasion assays

The Falcon[™] FluoroBlok HTS 24-Well Insert System (351,152; Corning, USA) and the ECMatrix Cell Invasion Assay (ECM554; MilliporeSigma, USA) were used, and the assays were performed as recommended. In brief, 1×10^5 cells suspended in serum-free culture medium were seeded in the upper chambers. DMEM supplemented with 10% FBS (11,960,044; Thermo Fisher Scientific, USA) was added to the lower chambers, and the plates were incubated for six hours at 37 °C and 5% CO₂. Cells migrating to the bottom surface of the insert membranes were dissociated from the membrane and detected by applying CyQUANT GR dye. The percentage of the fluorescence signal in the experimental groups relative to the control groups indicates the cell migration and invasion capabilities.

Flow cytometric analyses of apoptosis and the cell cycle

For apoptosis assays, approximately 1×10^5 UC cells were incubated with the components of an Annexin V-FITC kit (331200; Thermo Fisher, USA) at room temperature for 15 min and protected from light. For cell cycle assays,

UC cells were fixed in 70% ethanol overnight at -20 °C. Next, the cells were washed and resuspended in propidium iodide (PI)/ribonuclease staining buffer (550825; BD Biosciences, USA) for 15 min in the dark. These samples were then surveyed using a Novocyte[™] flow cytometer (ACEA Biosciences, USA). At least three independent experiments were carried out for each experimental group.

Human umbilical vein endothelial cells (HUVECs) tube formation assay

Fixed numbers (5×10^4 cells) of HUVECs (ATCC, USA) were incubated in the conditioned mediums collected from the *DPYSL3* knockdown and mock UC cells. They were then seeded in a 24-well plate precoated with Matrigel basement membrane matrix (Corning, USA). The experiment was terminated after six hours of incubation, and tube formation was analysed by measuring the tube formation ability on the images captured under high-quality phase-contrast microscopy.

Xenograft animal models

Stable BFTC909 *shLacZ* and *shDPYSL3#1* cells were mixed with high-concentration Matrigel (354248; Corning Life Sciences, USA) and injected subcutaneously into SCID Beige male mice (purchased from BioLASCO, Taiwan). The tumour size was recorded at the indicated time using an external calliper. The tumour volume was calculated using the following equation: Volume (mm³) = ($\pi/6$) × width (mm²) × length (mm). The mice were euthanized by CO₂ asphyxiation on Day 21. The excised tumours were fixed in 10% formalin for further analysis. This study was approved by the Institutional Animal Care and Use Committee of Chi-Mei Medical Center (Approval number 109041701).

Gene ontology (GO) enrichment analysis

The differentially expressed transcripts associated with *DPYSL3* overexpression in UC were identified using the BLCA dataset in TCGA. The analysis was performed online through the c-cBioPortal platform (<https://www.cbioportal.org/>). The top 500 genes that were positively and negatively coexpressed with *DPYSL3* were then subjected to GO enrichment analysis (<http://geneontology.org/>) to reveal the enriched biological processes.

Statistical analysis

All analyses were performed using IBM SPSS version 19 (IBM Corp, USA). The correlations between *DPYSL3* expression and clinicopathological features were assessed using the chi-square test. The impact of *DPYSL3* expression on patient outcomes was evaluated using Kaplan–Meier survival analysis. We performed a log-rank test to

analyse differences in survival. Disease-specific survival (DSS), metastasis-free survival (MFS), and local recurrence-free survival (LRFS) were selected as the clinical endpoints. DSS is the time elapsed from initial surgery to tumour-associated death. MFS is defined as the time from surgery to metastasis. LRFS is defined as the time from transurethral resection of the bladder tumour to tumour recurrence. A Cox proportional hazards regression model was developed to identify independent predictors for patient survival. Patients who were alive without events were censored at the last follow-up. A difference was considered significant if the p -value was ≤ 0.05 .

Results

DPYSL3 overexpression in UBUC was associated with tumour aggressiveness and poor patient survival

The GSE31684 dataset contains data for 93 UBUC patients. Eighty-four percent and thirty percent of these patients have MIBC and lymph node metastasis, respectively. Five transcripts (*DPYSL2*, *PAPSS2*, *DPYSL3*, *CILP*, and *GMPR*) associated with nucleobase-containing compound metabolic process (GO:0006139)

were correlated with UBUC invasiveness and metastasis (Fig. 1a and Table 1). Among these transcripts, *DPYSL3* had the highest log2 fold difference when comparing the MIBC vs. NMIBC groups (2.04-fold) and the distal metastasis events vs. no metastasis groups (0.77-fold). Correlation analysis with patient survival outcomes in the dataset revealed that *DPYSL3* was the only transcript that showed a significant survival impact in these patients ($p=0.005$, Figs. 1bi-v). We confirm this finding using the BCIA dataset from The Cancer Genome Atlas (TCGA) program. Analysis of the data online using Gene Expression Profiling Interactive Analysis (GEPIA) demonstrated that high *DPYSL3* expression predicts worse overall survival ($p=0.024$, Fig. 1bvi).

To confirm the in silico analysis results, we evaluated the relationship between *DPYSL3* mRNA expression levels in UBUC and tumour aggressiveness. The results showed that advanced-stage UBUC (pT2-pT4) had significantly higher *DPYSL3* mRNA expression than early-stage UBUC (pTa-pT1) ($p<0.001$, Fig. 1c). This result suggests that *DPYSL3* plays a significant role in urothelial carcinogenesis.

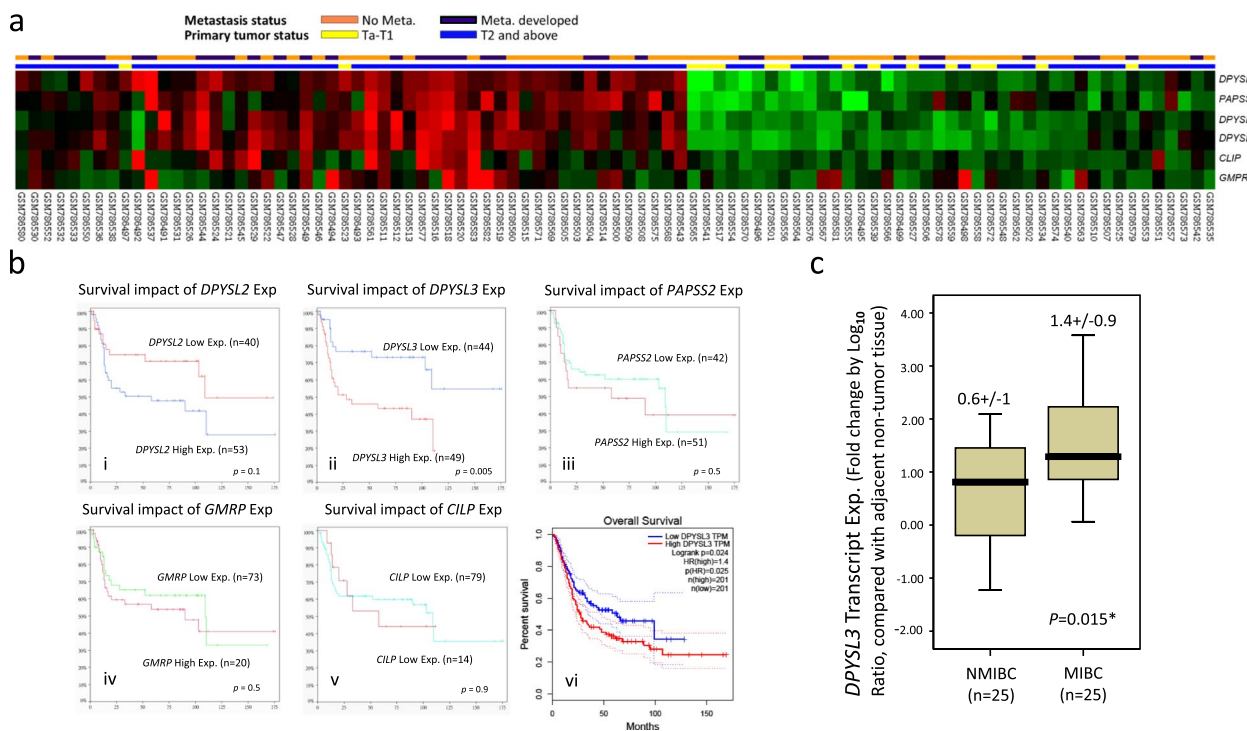


Fig. 1 In silico analyses of urinary bladder urothelial carcinoma (UBUC) datasets in the public domain. **a** Using the dataset, GSE32894, in Gene Expression Omnibus with a focus on the nucleobase-containing compound metabolic process (GO:0006139) term, a tumour cluster composed of mostly advanced-stage UBUC was found to have higher expression of five related transcripts (6 probes); **b** Of these transcripts, only (ii) *Dihydropyrimidinase-like 3* (*DPYSL3*) is significantly associated with survival ($p=0.005$); (vi) TCGA dataset analysis confirmed our finding; **c** We used 50 UBUC samples to validate this finding and showed higher *DPYSL3* mRNA levels in muscle-invasive bladder cancer than in non-muscle-invasive bladder cancer

Table 1 The significantly altered genes belong to the biological process GO:0006139

Probe	MIBC vs. NMIBC		Distal Meta. vs. Non-Meta ^{&}		Gene Symbol	Gene Title	Biological Process
	Log2 Ratio	p-Value	Log2 Ratio	p-Value			
200762_at	1.06	0.002*	0.62	0.016*	DPYSL2	dihydropyrimidinase-like 2	cell differentiation, multicellular organismal development, nervous system development, nucleobase; nucleoside; nucleotide and nucleic acid metabolic process, signal transduction
201430_s_at	1.21	<0.001*	0.34	0.015*	DPYSL3	dihydropyrimidinase-like 3	nervous system development, nucleobase; nucleoside; nucleotide and nucleic acid metabolic process, signal transduction
201431_s_at	2.04	<0.001*	0.77	0.002*	DPYSL3	dihydropyrimidinase-like 3	nervous system development, nucleobase; nucleoside; nucleotide and nucleic acid metabolic process, signal transduction
203060_s_at	1.34	<0.001*	0.58	0.037*	PAPSS2	3'-phosphoadenosine 5'-phosphosulfate synthase 2	nucleobase; nucleoside; nucleotide and nucleic acid metabolic process, skeletal development, sulfate assimilation
204187_at	0.15	0.045*	0.17	0.003*	GMPR	guanosine monophosphate reductase	metabolic process, nucleobase; nucleoside; nucleotide and nucleic acid metabolic process, nucleotide metabolic process, response to cold
206227_at	0.66	0.002*	0.54	<0.001*	CILP	cartilage intermediate layer protein; nucleotide pyrophosphohydrolase	nucleobase; nucleoside; nucleotide and nucleic acid metabolic process

MIBC muscle-invasive bladder cancer, NMIBC non-muscle invasive bladder cancer, Meta metastasis

* Statistically significant

[&] Development of subsequent metastasis

DPYSL3 protein overexpression is associated with aggressive clinicopathological features and results in poor survival outcomes in UBUC and UTUC

The DPYSL3 protein shows variable expression in UBUC and UTUC (Fig. 2 and Table 2). In UTUC, high DPYSL3 expression was associated with advanced-stage ($p < 0.001$), lymph node metastasis ($p < 0.001$), high histological grade ($p < 0.001$), vascular invasion ($p < 0.001$), perineural invasion ($p < 0.001$), and a high mitosis rate ($p < 0.001$). In patients with UBUC, increased expression of DPYSL3 was frequently related to muscle-invasive bladder cancer (MIBC) ($p < 0.001$), lymph node metastasis ($p = 0.012$), vascular invasion ($p < 0.001$), and perineural invasion ($p = 0.021$). These observations indicate the importance of DPYSL3 in promoting UC aggressiveness.

The univariable and multivariable analysis results of the clinicopathological features are listed in Tables 3, 4 and 5. For UTUC patients (median (interquartile range (IQR)) follow-up time = 38.2 (19.8, 65.7) months), nodal metastasis and perineural invasion are important clinicopathological factors independently correlated with DSS and MFS. In addition, the histological grade is an independent prognostic factor for DSS and multifocality for MFS.

For UBUC patients (median (IQR) follow-up time = 23.4 (9.9, 43.2) months), the primary tumour stage (pT) and mitotic rate predict DSS and MFS of patients. Although univariable analysis showed that pT ($p = 0.019$) and histological grade ($p = 0.01$) are correlated with LRFS in NMIBC patients after transurethral resection of bladder tumours (TURBT), they are not independent prognostic factors (Table 5).

Patients with UTUC expressing higher levels of DPYSL3 had a significantly higher death rate (31.8% vs. 4.1%, $p < 0.001$) and more frequent metastatic events (35.3% vs. 3.5%, $p < 0.001$, Table 3). In addition, DPYSL3 overexpression was an independent prognostic factor for both DSS ($p = 0.005$) and MFS ($p < 0.001$, Table 3 and Figs. 3a and b). DPYSL3 expression also has a similar effect on UBUC. A higher death rate (29.7% vs. 5.4%, $p < 0.001$) and frequent metastasis (43.2% vs. 7.5%, $p < 0.001$) are seen in UBUC with high DPYSL3 expression (Table 4). Besides, high expression of DPYSL3 also independently predicts dismal DSS ($p < 0.001$) and MFS ($p < 0.001$) outcomes in UBUC patients (Table 4 and Figs. 3a-d). For NMIBC patients, DPYSL3 overexpression was significantly correlated with local recurrence

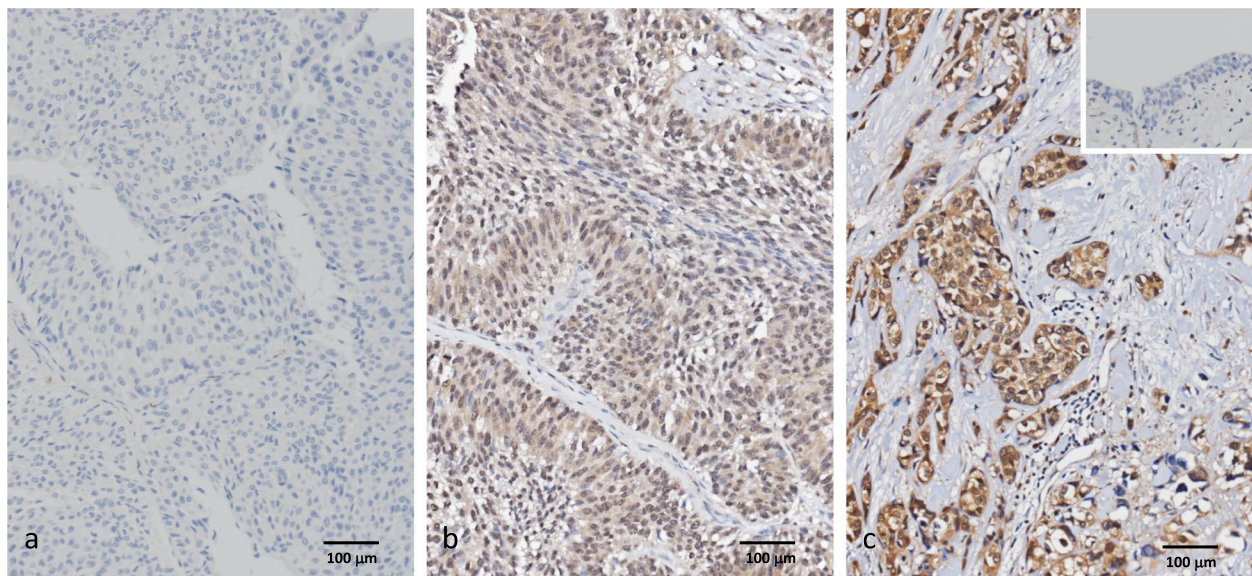


Fig. 2 Dihydropyrimidinase-like 3 (DPYSL3) immunohistochemical staining in various stages of urothelial carcinoma. **a** A noninvasive papillary urothelial carcinoma (pTa) is negative for DPYSL3; **b** an early invasive urothelial carcinoma (pT1) shows a low to moderate degree of DPYSL3 expression; **c** a muscle-invasive bladder carcinoma (> pT2, MIBC) shows diffuse, strong DPYSL3 expression. (Magnification, 200×)

Table 2 Correlations between dihydropyrimidinase-like 3 (DPYSL3) expression and other important clinicopathological parameters in urothelial carcinomas

Parameter	Category	Upper Urinary Tract Urothelial Carcinoma				Urinary Bladder Urothelial Carcinoma			
		Case No	DPYSL3 Expression		p-Value	Case No	DPYSL3 Expression		p-Value
			Low	High			Low	High	
Gender	Male	158	75	83	0.4	216	106	110	0.7
	Female	182	95	87		79	41	38	
Age (years)	< 65	138	70	68	0.8	121	55	66	0.2
	≥ 65	202	100	102		174	92	82	
Tumour location	Renal pelvis	141	66	75	0.2	-	-	-	-
	Ureter	150	83	67		-	-	-	-
	Renal pelvis & ureter	49	21	28		-	-	-	-
Multifocality	Single	278	143	135	0.3	-	-	-	-
	Multifocal	62	27	35		-	-	-	-
Primary tumour (T)	Ta	89	71	18	< 0.001*	84	54	30	< 0.001*
	T1	92	54	38		88	47	41	
	T2–T4	159	45	114		123	46	77	
Nodal metastasis	Negative (N0)	312	168	144	< 0.001*	266	139	127	0.012*
	Positive (N1–N2)	28	2	26		29	8	21	
Histological grade	Low grade	56	44	12	< 0.001*	56	33	23	0.1
	High grade	284	126	158		239	114	125	
Vascular invasion	Absent	234	153	81	< 0.001*	246	137	109	< 0.001*
	Present	106	17	89		49	10	39	
Perineural invasion	Absent	321	169	152	< 0.001*	275	142	133	0.021*
	Present	19	1	18		20	5	15	
Mitotic rate (per 10 high power fields)	< 10	173	110	63	< 0.001*	139	73	66	0.4
	≥ 10	167	60	107		156	74	82	

* Statistically significant; RR relative risk

Table 3 Univariable and multivariable analyses for disease-specific and metastasis-free survivals in upper urinary tract urothelial carcinoma

Parameter	Category	Case No	Disease-Specific Survival			Metastasis-Free Survival						
			Univariable Analysis		Multivariable Analysis	Univariable Analysis		Multivariable Analysis				
			No. of Event	p-Value	RR	95% CI	p-Value	No. of Event	p-Value	RR	95% CI	p-Value
Gender	Male	158	28	0.8	-	-	-	32	0.8	-	-	-
	Female	182	33	-	-	-	-	38	-	-	-	-
Age (years)	<65	138	26	1	-	-	-	30	0.8	-	-	-
	≥65	202	35	-	-	-	-	40	-	-	-	-
Tumour side	Right	177	34	0.7	-	-	-	38	0.3	-	-	-
	Left	154	26	-	-	-	-	32	-	-	-	-
Tumour location	Bilateral	9	1	-	-	-	0	-	-	-	-	-
	Renal pelvis	141	24	0.008*	-	-	31	0.1	-	-	-	-
	Ureter	150	22	-	-	-	25	-	-	-	-	-
	Renal pelvis & ureter	49	15	-	-	-	14	-	-	-	-	-
Multifocality	Single	273	48	0.003*	-	-	52	0.013*	-	-	-	0.007*
	Multifocal	62	18	-	-	-	18	-	-	2.2	1.2, 3.8	-
Primary tumour (T)	Ta	89	2	<0.001*	1	-	4	<0.001*	-	1	-	0.3
	T1	92	9	-	1.7	0.7, 3.8	15	-	-	2.5	0.8, 7.9	-
	T2–T4	159	50	-	5.4	1.2, 25	51	-	-	2.1	0.7, 6.7	-
Nodal metastasis	Negative (N0)	312	42	<0.001*	1	-	55	<0.001*	-	1	-	0.002*
	Positive (N1–N2)	28	19	-	3.6	2.1, 6.5	15	-	-	2.6	1.4, 4.9	-
Histological grade	Low grade	56	4	0.022*	-	-	3	0.003*	-	1	-	0.1
	High grade	284	57	-	-	-	67	-	-	1.9	0.8, 4.1	-
Vascular invasion	Absent	234	24	<0.001*	1	-	26	<0.001*	-	1	-	0.1
	Present	106	37	-	1.3	0.7, 2.4	44	-	-	1.8	0.1, 3.3	-
Perineural invasion	Absent	321	50	<0.001*	1	-	61	<0.001*	-	1	-	0.048*
	Present	19	11	-	2.6	1.7, 7.4	9	0.1	-	2.1	1, 4.4	-
Mitotic rate (per 10 high power fields)	<10	173	27	0.2	-	-	30	-	-	-	-	-
	>=10	167	34	-	-	-	40	-	-	-	-	-
DPYSL3 expression	Low	170	7	<0.001*	1	-	6	<0.001*	-	1	-	<0.001*
	High	170	54	-	3.4	1.5, 8.1	64	-	-	6.2	2.5, 15	-

* Statistically significant; RR relative risk

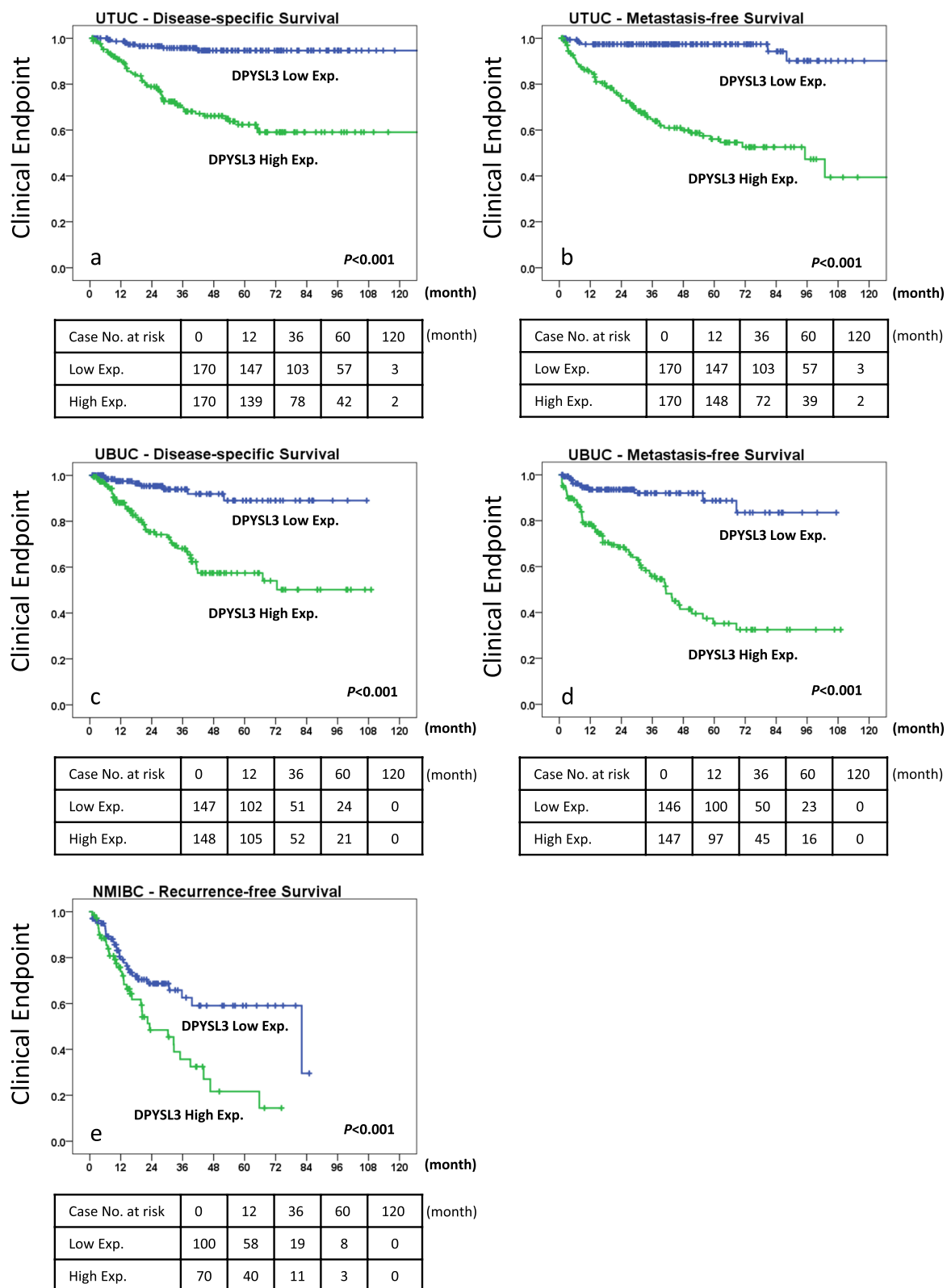


Fig. 3 Kaplan–Meier analyses of survival based on Dihydropyrimidinase-like 3 (DPYSL3) expression in urothelial carcinoma. The plots show that DPYSL3 overexpression is correlated with inferior (a) disease-specific survival (DSS) and (b) metastasis-free survival (MFS) outcomes in patients with upper urinary tract urothelial carcinoma (UTUC); c, d a similar pattern is also observed in patients with urinary bladder urothelial carcinoma (UBUC); e in patients with non-muscle-invasive UBUC, high DPYSL3 expression is correlated with a higher local recurrence-free survival (LRFS) rate

Table 4 Univariable and multivariable analyses for disease-specific and metastasis-free survivals in urinary bladder urothelial carcinoma

Parameter	Category	Case No	Disease-Specific Survival				Metastasis-Free Survival				
			Univariable Analysis		Multivariable Analysis		Univariable Analysis		Multivariable Analysis		
			No. of Event	p-Value	RR	95% CI	p-Value	95% CI	RR	95% CI	p-Value
Gender	Male	216	41	0.4	-	-	-	60	0.3	-	-
	Female	79	11	-	-	-	-	16	-	-	-
Age (years)	< 65	121	17	0.1	-	-	-	31	0.7	-	-
	≥ 65	174	35	-	-	-	-	45	-	-	-
Primary tumour (T)	Ta	84	1	<0.001*	1	-	<0.001*	4	<0.001*	1	-
	T1	88	9	-	4.1	1.9,9.2	-	23	-	4	1.2,14
	T2-T4	123	42	-	32	4.3,250	-	49	-	5.8	1.6,20
Nodal metastasis	Negative (N0)	266	41	<0.001*	1	-	0.6	61	<0.001*	1	-
	Positive (N1-N2)	29	11	-	1.2	0.6,2.4	-	15	-	1.7	0.9,3.2
Histological grade	Low grade	56	2	0.001*	-	-	-	5	<0.001*	1	-
	High grade	239	50	-	-	-	-	71	-	1.5	0.5,4.1
Vascular invasion	Absent	246	37	0.002*	1	-	0.1	54	<0.001*	1	-
	Present	49	15	-	0.5	0.3,1	-	22	-	0.8	0.4,1.4
Perineural invasion	Absent	275	44	<0.001*	1	-	0.1	66	<0.001*	1	-
	Present	20	8	-	2.2	1,5.3	-	10	-	1.6	0.7,3.3
Mitotic rate (per 10 high power fields)	< 10	139	12	<0.001*	-	-	-	23	<0.001*	1	-
	> = 10	156	40	-	-	-	-	53	-	1.7	1,2.9
DPY5L3 expression	Low	147	8	<0.001*	1	-	<0.001*	11	<0.001*	1	-
	High	148	44	-	4	1.8,8.6	-	64	-	5.1	2.7,9.9

* Statistically significant; RR relative risk

Table 5 Univariable and multivariable analyses for local recurrence-free survivals in non-muscle-invasive bladder carcinoma

Parameter	Category	Case No	Local Recurrence-Free Survival				
			Univariable Analysis		Multivariable Analysis		
			No. of Event	p-Value	RR	95% CI	p-Value
Gender	Male	125	46	0.3	-	-	-
	Female	47	19		-	-	-
Age (years)	< 65	70	30	0.4	-	-	-
	≥ 65	102	35		-	-	-
Primary tumour (T)	Ta	84	27	0.019*	1	-	0.8
	T1	88	38		1	0.6, 2	
Nodal metastasis	Negative (N0)	172	65	n.a	-	-	-
	Positive (N1–N2)	0	0		-	-	-
Histological grade	Low grade	54	15	0.01*	1	-	0.1
	High grade	118	50		2	1, 4.2	
Vascular invasion	Absent	171	65	0.7	-	-	-
	Present	1	0		-	-	-
Perineural invasion	Absent	169	64	0.5	-	-	-
	Present	3	1		-	-	-
Mitotic rate (per 10 high power fields)	< 10	94	35	0.2	-	-	-
	> = 10	78	30		-	-	-
DPYSL3 expression	Low	101	29	0.004*	1	-	0.01*
	High	71	36		2	1.2, 3.3	

* Statistically significant; RR relative risk

(26.8% vs. 1.0%, $p=0.005$). DPYSL3 also independently predicted the LRFS ($p=0.01$) in NMIBC patients after TURBT (Table 5 and Fig. 3e).

DPYSL3 mRNA interference reverses UC cell proliferation and aggressiveness

We screened UC cell lines (T24, TCCSUP, RT4, BFTC909, BFTC905, and UMUC3) to understand the expression level of the DPYSL3 transcript. BFTC909 and T24 have high DPYSL3 transcript levels among these UC cell lines. Western blots confirmed that the corresponding protein levels were equally elevated (Figs. 4a and S1). To generate stable clones of UC cells with low DPYSL3 expression, we infected BFTC909 and T24 cells with lentivirus carrying shDPYSL3 to knock down DPYSL3 expression (Figs. 4b, S1 and S2).

After DPYSL3 knockdown, UC cells exhibited a significantly decreased proliferation ability (both $p < 0.05$, Fig. 4c). The DPYSL3 knockdown clones (KD clones) also showed a higher apoptosis rate (BFTC909 $p < 0.05$; T24 not significant, Fig. 4d) and an increased G0/G1 fraction (both $p < 0.05$, Fig. 4e and Table S2). These results suggest that DPYSL3 facilitates UC cell proliferation by positively regulating cell cycle progression and preventing apoptosis. Furthermore, KD clones significantly decreased the migration and invasion ability of BFTC909 and T24 cells (Figs. 5a and b). In addition, the KD clones also exhibited a significantly decreased HUVECs tube formation ability (Fig. 5c). These findings suggested that DPYSL3 enhanced the migration and invasion abilities of UC cells and promoted angiogenesis in UC.

(See figure on next page.)

Fig. 4 Dihydropyrimidinase-like 3 (DPYSL3) knockdown increased urothelial carcinoma (UC) cells apoptosis and altered the cell cycle. **a** T24 and BFTC909 are among the UC cells with increased DPYSL3 mRNA transcript and high DPYSL3 protein expression; **b** T24 and BFTC909 cells infected with lentivirus carrying DPYSL3 shRNA exhibited successful knockdown of DPYSL3 expression; **c** DPYSL3 knockdown UC cells have a significantly decreased proliferation ability ($p < 0.05$); **d** DPYSL3 knockdown T24 cells showed a trend toward an increase in apoptotic activity, and apoptosis was significantly increased in DPYSL3 knockdown BFTC909 cells ($p < 0.05$); **e** DPYSL3 knockdown UC cells exhibited a significantly increased G0/G1 fraction ($p < 0.05$)

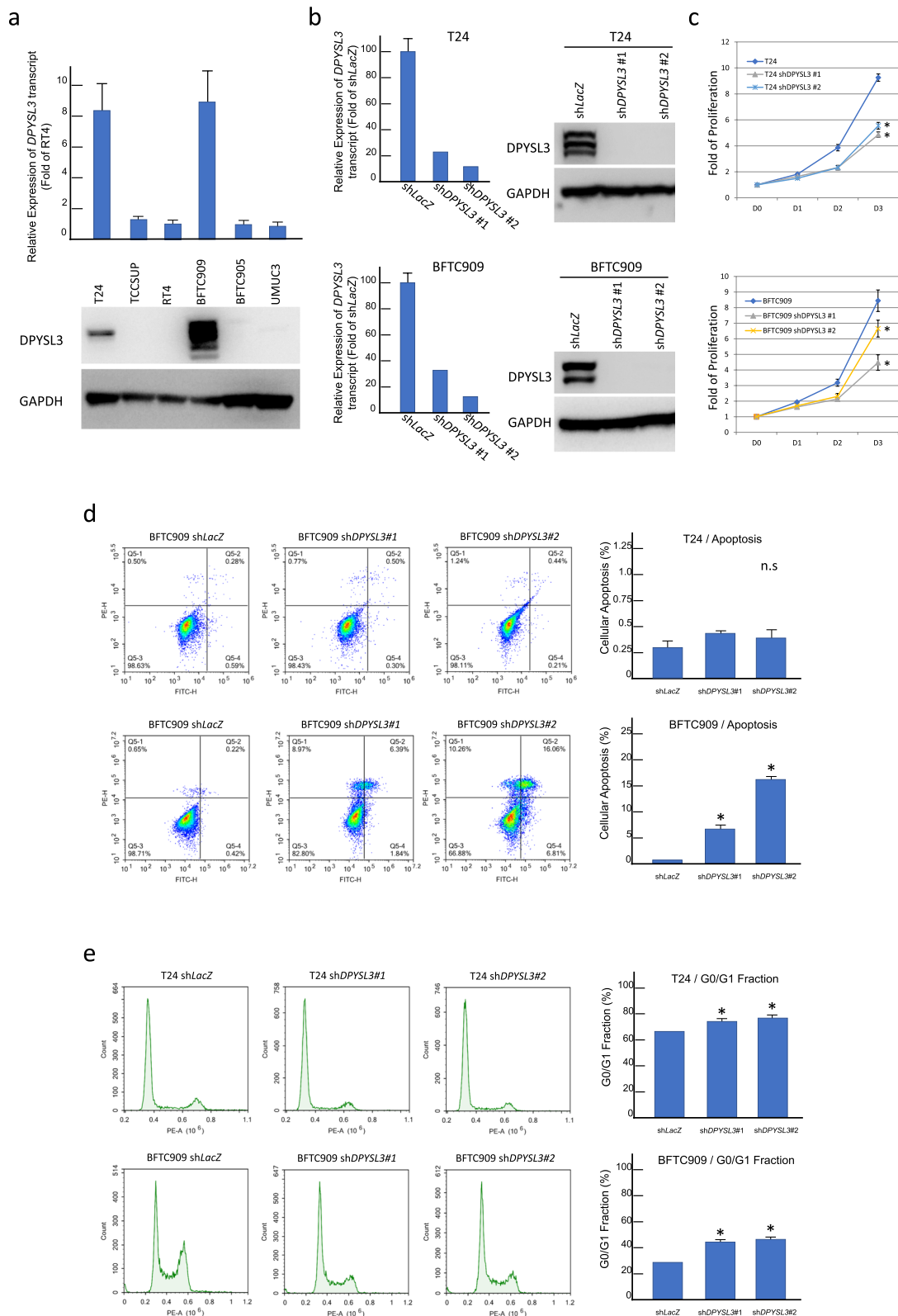


Fig. 4 (See legend on previous page.)

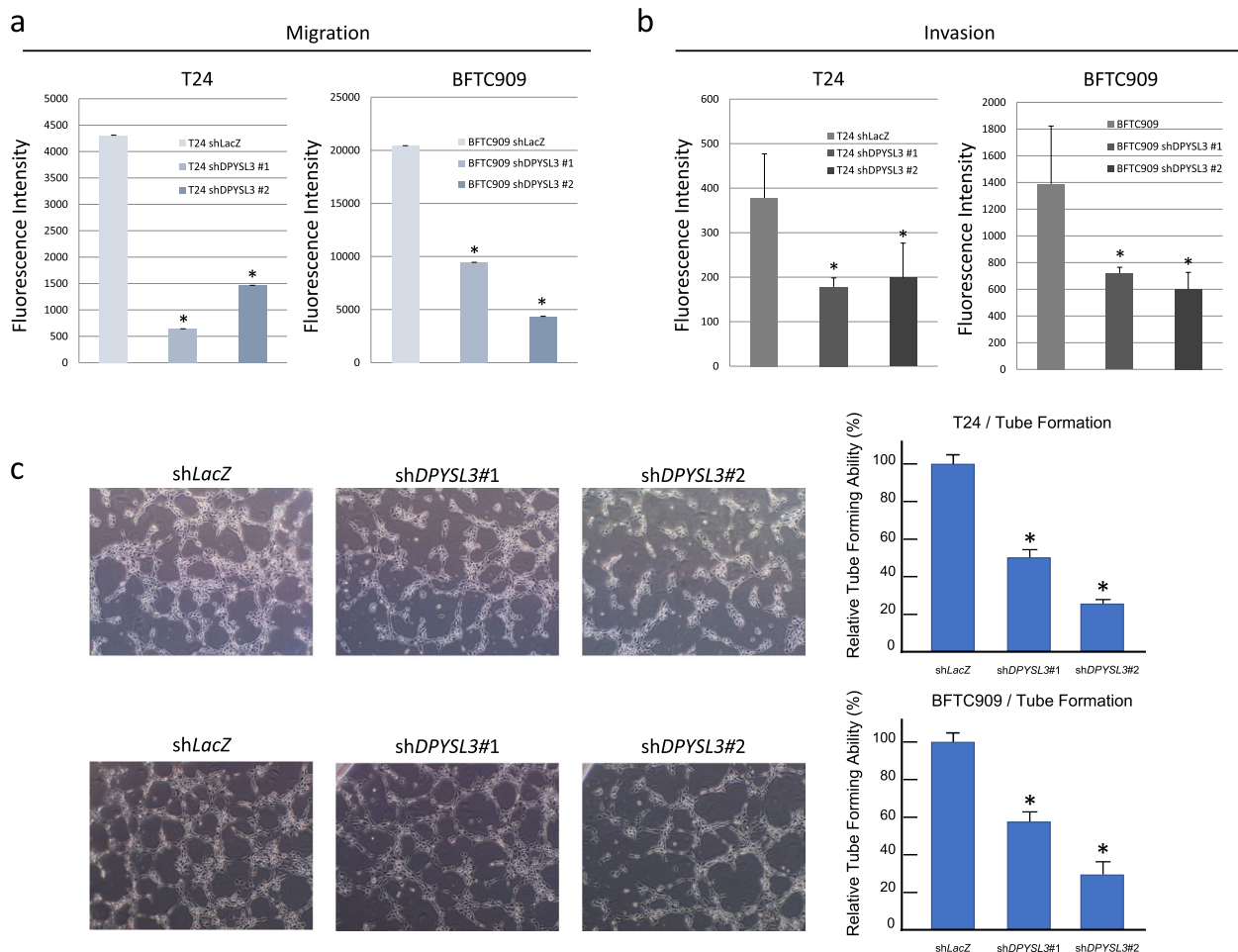


Fig. 5 Dihydropyrimidinase-like 3 (DPYSL3) knockdown suppressed urothelial carcinoma (UC) cell migration/invasion and hampered angiogenesis. The plots show that UC cells with DPYSL3 knockdown had a significantly suppressed (a) migration ability and (b) invasion ability ($p < 0.05$); c human umbilical vein endothelial cells (HUVECs) tube formation was significantly hampered after culture in the conditioned medium of DPYSL3-knockdown UC cells ($p < 0.05$)

Genes coexpressed with DPYSL3 in UC are correlated with cell migration, mesenchymal remodelling, and metabolic processes

The 500 transcripts whose levels were most significantly positively or negatively correlated with the DPYSL3 mRNA level in the BLCA dataset of TCGA were extracted and are listed in Tables S3 and S4, respectively. The biological processes involving these genes identified by GO enrichment analysis are displayed in Tables S5 and S6. The top 10 positively associated genes were *MSRB3*, *BNC2*, *CALD1*, *FXYD6*, *FERMT2*, *FGFR1*, *PDLIM3*, *MIR100HG*, *MYLK*, and *TGFB3*. The top 10 biological processes enriched with the positively associated transcripts included “aorta smooth muscle tissue morphogenesis (GO:0060414)”, “mesenchyme migration (GO:0090131)”, “hematopoietic stem cell migration to bone marrow (GO:0097241)”, “elastic fiber assembly (GO:0048251)”, “intramembranous

ossification (GO:0001957)”, “relaxation of vascular associated smooth muscle (GO:0060087)”, “direct ossification (GO:0036072)”, “lung growth (GO:0060437)”, “regulation of Rho-dependent protein serine/threonine kinase activity (GO:2000298)”, and “relaxation of smooth muscle (GO:0044557)”. On the other hand, the top 10 genes negatively associated with DPYSL3 were *PLEKHH1*, *MAP7*, *OVOL1*, *ID1*, *CRB3*, *ESRRA*, *DTX4*, *CHMP4C*, *SSH3*, and *SLC22A5*. The top 10 biological processes enriched with the negatively associated transcripts were “tRNA processing (GO:0008033)”, “regulation of RNA splicing (GO:0043484)”, “fatty acid metabolic process (GO:0006631)”, “mRNA processing (GO:0006397)”, “mRNA metabolic process (GO:0016071)”, “carboxylic acid metabolic process (GO:0019752)”, “oxoacid metabolic process (GO:0043436)”, “organic acid metabolic process (GO:0006082)”, “RNA processing (GO:0006396)”, and “cellular lipid metabolic process (GO:0044255)”.

DPYSL3 mRNA interference in UC cells suppressed mTOR signalling

The PI3K/AKT/mTOR pathway is essential in regulating energy homeostasis and is frequently affected in UC [31, 32]. Since genes associated with *DPYSL3* were enriched in energy-metabolism processes, we hypothesized that knocking down *DPYSL3* in UC cells suppressed mTOR signalling. Immunoblot analysis revealed that KD clones had decreased the protein levels of mTOR, phospho-RPS6 (p-RPS6(S235)), and MYC (Fig. 6a). The expression of AKT, phospho-AKT (p-AKT(S473)), and phospho-mTOR (p-MTOR(S2448)) was decreased in shDPYSL3#1 T24 cells but not in shDPYSL3#1 BFTC909. Although the active/phospho-mTOR is not consistently suppressed, the downregulation of phospho-RPS6 upon *DPYSL3* knockdown indicated that the mTORC1 activity was affected. These findings suggested that *DPYSL3* can enhance mTORC1 signalling in UC cells, which would be predicted to promote aerobic glycolysis. In addition, *DPYSL3* confers UC aggressiveness is associated with activating the mTOR pathways and cMYC overexpression.

DPYSL3 knockdown UC cells downregulated GLUT1 expression and hampered tumour growth in vivo

The mTOR pathway is a vital regulator in cancer cells to induce aerobic glycolysis, a crucial feature in UBUC [33, 34]. Immunoblot analysis revealed that *DPYSL3* knockdown in BFTC909 and T24 significantly suppressed GLUT1 expression but did not affect HK2 and LDHA/C expression (Fig. 6a). These findings indicate that *DPYSL3* stimulated glucose influx through increased GLUT1 expression, fuelling the mTOR signal.

The mouse xenograft experiments showed that the growth of tumours derived from BFTC909 cells was hampered after *DPYSL3* knockdown. The average tumour size was significantly smaller in the BFTC909 shDPYSL3 group than in the BFTC909 shLacZ group ($p < 0.05$, Figs. 6b and c). The tumours developed from BFTC909 shDPYSL3 cells had lower cMYC and GLUT1 expression (Fig. 6d). Based on these findings, we revealed that *DPYSL3* could promote rapid UC growth by cMYC overexpression and increased glucose influx in UC. The link between *DPYSL3* and cancer energy metabolism has never been reported and thus warrants further investigation.

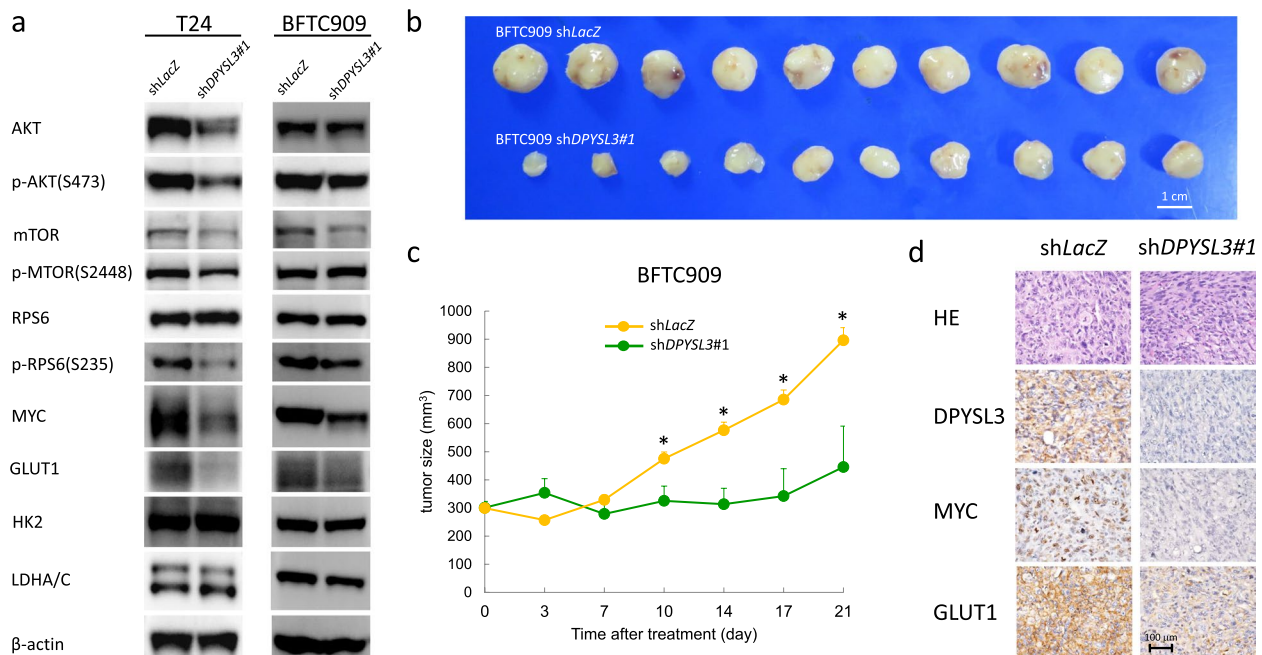


Fig. 6 Dihydropyrimidinase-like 3 (*DPYSL3*) knockdown increased phosphorylation of mTORC1 and enhanced UC tumour aggressiveness. The relationship between *DPYSL3* and proteins associated with the mTOR pathway was explored by Western blot analysis. **a** p-mTOR, p-RPS6(S235), Myc, and Glut1 were consistently and significantly downregulated in T24 and BFTC909 with *DPYSL3* knockdown. **b** BFTC909-derived xenograft model ($n = 10$ for each group) confirmed the effects of *DPYSL3* on promoting tumour growth. **c** The growth rate of tumours derived from shDPYSL3#1 BFTC909 cells was significantly lower than those derived from shLacZ BFTC909 cells in SCID Beige mice. **d** IHC analysis of xenografted samples at day 21 post-inoculation showed that the expression of *DPYSL3*, MYC, and GLUT1 was suppressed in the *DPYSL3* knockdown group, in contrast to the control group (Magnification, 400 \times). Data are shown as the mean \pm SEM. Statistical significance: $*p < 0.05$

Discussion

Rapid growth and sustained proliferation are hallmarks of malignant tumours [35]. To maintain expedited cell cycle progression, a continually replenished nucleotide pool is required to support DNA and RNA synthesis. The metabolic shift to a higher de novo nucleotide synthesis rate is thus crucial to supporting tumour development and progression [36]. Upon data mining of the GEO dataset GSE31684, we found that DPYSL3 expression was significantly correlated with UBUC patient prognosis in a manner focused on the nucleobase-containing compound metabolic process (GO:0006139). Analyses with our well-documented cohorts confirmed that increased DPYSL3 protein expression in UTUC and UBUC is associated with poor DFS and MFS. In addition, high DPYSL3 expression predicted a higher bladder tumour recurrence rate in patients with NMIBC. This finding suggests that DPYSL3 positively affects tumour aggressiveness and plays an essential role in the tumorigenesis of UC.

Activation of invasion and metastasis is one of the hallmark capabilities of cancer cells. Cancer cells have two distinct modes of invasion: “collective invasion” and “single-cell migration” [35]. The former is characterized by the invasive growth of whole groups of tumour cells into adjacent tissue interconnected by adhesion molecules and communication junctions [37, 38]. The latter is characterized by the invasion of individual tumour cells into the surrounding stroma [38]. Dynamic modification of the actin cytoskeleton is required for cell migration, playing a vital role in the invasion and metastasis of cancer cells [39]. In claudin-low breast cancer cells, DPYSL3 mRNA and the epithelial-mesenchymal transition (EMT) markers SNAIL and TWIST can regulate each other reciprocally [40]. In addition, DPYSL3-silenced lung cancer cells overexpress epithelial markers and down-regulated mesenchymal markers [24]. Since our in vitro and in vivo results revealed that DPYSL3 increased UC aggressiveness by promoting tumour cell proliferation, migration, and invasion, it is possible that DPYSL3 confers aggressive behaviours on UC cells through profound modulation of the UC cell actin cytoskeleton, boosts epithelial-mesenchymal transition, and promotes cell mitosis.

In addition to modifying UC cell invasiveness, DPYSL3 is involved in diverse molecular processes to promote tumour aggressiveness. Our experiment showed that DPYSL3 knockdown in UC not only promotes G1-phase arrest but also enhances UC cell apoptosis. A previous study in gastric cancer showed that modulating the expression of the short DPYSL3 isoform induces G1-phase arrest but not apoptosis [41]. In addition, decreased DPYSL3 expression in UC cells suppressed tumour angiogenesis. Our previous study has shown

that an increased microvascular density in UC tumours is associated with poor patient survival outcomes [42]. DPYSL3 could be used as a biomarker to identify patients most likely to benefit from antiangiogenic therapeutics. The mechanism of DPYSL3-promoted angiogenesis in UC is still unknown, but a previous study showed that the expression of DPYSL3 and VEGF was correlated [20].

Metabolic reprogramming (the Warburg effect) is critical for cancer cell proliferation. In addition to rapid ATP synthesis, metabolic process remodelling supports the biosynthetic pathways and promotes signalling transduction crucial for cancer cells [43]. Alterations in the metabolic pathway can promote tumorigenesis and EMT [44, 45]. From the Gene Ontology analysis, we discovered that genes associated with DPYSL3 were also enriched in functions related to metabolic processes. We revealed that DPYSL3 overexpression correlates with increased MYC and GLUT-1 expression using a mouse xenograft model. We also demonstrated that DPYSL3 expression correlates with mTOR pathway activation in UC cell lines. mTOR induces metabolic reprogramming in tumours by boosting protein and lipid synthesis and aerobic glycolysis to fuel tumour cells [46]. Based on the findings, we suggested that DPYSL3 induced GLUT1 expression in UC cells, which led to glucose influx into the cells. Increased intracellular glucose can activate mTORC1 by increasing Rheb interaction [47]. With the upregulated cMYC induced by DPYSL3, mTORC1 reprogrammed UC metabolism by promoting glutaminolysis, glycolysis, and nucleotide synthesis [48].

This study had two significant limitations that must address in future studies. First, this is a single institute study, and the tissue samples collected are from a region where UTUC has a high prevalence. The etiology of UC development may be, and therefore, our findings might not apply to different populations. A multicenter, multi-continental study will be needed to confirm our observations. Second, our result only demonstrated that UC with DPYSL3 knockdown is associated with decreased MYC and GLUT1 expression; how DPYSL3 promotes energy reprogramming has yet to clarify. Reduced phosphorylation of mTOR and RPS6 may be essential for DPYSL3 in altering the energy metabolism of UC. A comprehensive study on DPYSL3 interaction with tumour cell energy metabolism will be needed to understand the underlying molecular mechanism. Despite this limitation, our study is the first to disclose DPYSL3 in reprogramming energy metabolism in cancer development.

Conclusions

DPYSL3 is an important biomarker that correlates with UC aggressiveness and independently predicts UTUC and UBUC outcomes. The oncogenic roles of DPYSL3

in UC involved cytoskeleton modification, promoting cell proliferation, preventing apoptosis, induced angiogenesis, and reprogramming metabolic processes. DPYSL3 confers tumour aggressiveness by increased cMYC and GLUT1 expression and activation of mTORC1 signalling. DPYSL3 could serve as a prognostic marker and a potential therapeutic target for UC.

Abbreviations

CLOW	Claudin-low
CRMP4	Collapsing response mediator protein 4
DPYSL3	Dihydropyrimidinase-like 3 protein
DSS	Disease-specific survival
EMT	Epithelial-mesenchymal transition
FFPE	Formalin-fixed paraffin-embedded
GEO	Gene Expression Omnibus
GEPIA	Gene Expression Profiling Interactive Analysis
GO	Gene Ontology
GSK3b	Glycogen synthase kinase 3 beta
HUVECs	Human umbilical vein endothelial cells
LRFS	Local recurrence-free survival
MFS	Metastatic free survival
MIBC	Muscle-invasive bladder cancer
NMIBC	Non-muscle invasive bladder cancer
pT	Primary tumour stage
TCGA	The Cancer Genome Atlas
TMA	Tissue microarrays
UBUC	Urinary bladder urothelial carcinoma
UC	Urothelial carcinoma
UTUC	Upper urinary tract urothelial carcinoma
VEGF	Vascular epithelial growth factor

Supplementary Information

The online version contains supplementary material available at <https://doi.org/10.1186/s12885-023-11090-z>.

Additional file 1: Table S1. Primary antibodies and dilution for immunohistochemistry and immunoblot analysis.

Additional file 2: Table S2. The flow cytometry assay of the Cell Cycle of mock and DPYSL3 knockdown UC cells (BFTC909 and T24).

Additional file 3: Figs. S1–S7. Immunoblot Gel Raw data.

Additional file 4: Table S3. The top 500 most significant differentially expressed genes positively correlated with *DPYSL3* expression in bladder cancer.

Additional file 5: Table S4. The top 500 most significant differentially expressed genes negatively correlated with *DPYSL3* expression in bladder cancer.

Additional file 6: Table S5. GO enrichments of positively associated genes.

Additional file 7: Table S6. GO enrichments of negatively associated genes.

Acknowledgements

Not applicable

Authors' contributions

Conception and design: P.-I. L., Y.-H. K. and C.-F. L.; collect samples and data acquisition: H.-Y. L., T.-C. C., C.-H. H., SK H., K.-L. H., W.-H. T., T.-J. C., W.-S. L., Y.-H. K., and C.-F. L.; analysis and interpretation of data: P.-I. L., H.-Y. L., T.-C. C., and W.-M. L.; statistical analysis: C.-F. L.; drafting of the manuscript: P.-I. L., H.-D. C., and C.-F. L.; critical revision of the manuscript: P.-I. L., H.-Y. L., T.-C. C., Y.-H. K., H.-D. C.,

and C.-F. L. All authors have read and agreed to the published version of the manuscript.

Funding

This research was funded by Kaohsiung Medical University Hospital, Kaohsiung Medical University, Taiwan (KMUH107-7M39), and the Ministry of Science and Technology, Taiwan (MOST108-2320-B-037-027-).

Availability of data and materials

The datasets generated and analyzed during the current study are not publicly available since the storage of the data in a public register is not covered by the patient's declaration of consent. However, an anonymous data set is available from the corresponding author [C.-F. L.] on reasonable request.

Declarations

Ethics approval and consent to participate

This study was approved by the Institutional Review Board of the Chi Mei Medical Center (IRB10501-005). Informed consent was obtained from all subjects involved in the study. All methods were performed in accordance with the relevant guidelines and regulations. The animal experiment was approved by the Institutional Animal Care and Use Committee of Chi-Mei Medical Center (Approval number 109041701). All experimental procedures were conducted in compliance with institutional guidelines and regulations. All studies involving animals are reported in accordance with the ARRIVE guidelines.

Consent for publication

Not applicable

Competing interests

The authors declare no competing interests.

Author details

¹Department of Pathology, Kaohsiung Medical University Hospital, Kaohsiung Medical University, Kaohsiung 807378, Taiwan. ²Department of Medical Research, Chi Mei Medical Center, Tainan 710402, Taiwan. ³National Institute of Cancer Research, National Health Research Institutes, Tainan 704016, Taiwan. ⁴Department of Urology, Kaohsiung Medical University Hospital, Kaohsiung Medical University, Kaohsiung 807378, Taiwan. ⁵Department of Urology, School of Medicine, College of Medicine, Kaohsiung Medical University, Kaohsiung 807378, Taiwan. ⁶Center for Liquid Biopsy and Cohort Research, Kaohsiung Medical University, Kaohsiung 807378, Taiwan. ⁷Department of Urology, Ministry of Health and Welfare Pingtung Hospital, Pingtung 90054, Taiwan. ⁸Department of Anesthesiology, Chi Mei Medical Center, Tainan 710402, Taiwan. ⁹Department of Surgery, Division of Urology, Chi Mei Medical Center, Tainan 710402, Taiwan. ¹⁰Department of Medical Science Industries, College of Health Sciences, Chang Jung Christian University, Tainan 711301, Taiwan. ¹¹Department of Clinical Pathology, Chi Mei Medical Center, Tainan 710402, Taiwan. ¹²Department of Medical Technology, Chung Hwa University of Medical Technology, Tainan 71703, Taiwan. ¹³Department of Pathology, Chi Mei Medical Center, Tainan 710402, Taiwan. ¹⁴Department of Internal Medicine, Division of Hematology and Oncology, Chi-Mei Medical Center, Tainan 710402, Taiwan. ¹⁵College of Pharmacy and Science, Chia Nan University, Tainan 71710, Taiwan.

Received: 16 June 2022 Accepted: 20 June 2023

Published online: 28 June 2023

References

- Wong MCS, Fung FDH, Leung C, Cheung WWL, Goggins WB, Ng CF. The global epidemiology of bladder cancer: a joinpoint regression analysis of its incidence and mortality trends and projection. *Sci Rep*. 2018;8:1129.
- Giudici N, Bonne F, Blarer J, Minoli M, Krentel F, Seiler R. Characteristics of upper urinary tract urothelial carcinoma in the context of bladder cancer: a narrative review. *Transl Androl Urol*. 2021;10:4036–50.

3. Soria F, Shariat SF, Lerner SP, Fritsche HM, Rink M, Kassouf W, et al. Epidemiology, diagnosis, preoperative evaluation and prognostic assessment of upper-tract urothelial carcinoma (UTUC). *World J Urol.* 2017;35:379–87.
4. Dickman KG, Chen CH, Grollman AP, Pu YS. Aristolochic acid-containing Chinese herbal medicine and upper urinary tract urothelial carcinoma in Taiwan: a narrative review. *World J Urol.* 2023;41:899–907.
5. Lobo N, Afferi L, Moschini M, Mostafid H, Porten S, Psutka SP, et al. Epidemiology, screening, and prevention of bladder cancer. *Eur Urol Oncol.* 2022;5:628–39.
6. Rink M, Ehdäie B, Cha EK, Green DA, Karakiewicz PI, Babjuk M, et al. Stage-specific impact of tumor location on oncologic outcomes in patients with upper and lower tract urothelial carcinoma following radical surgery. *Eur Urol.* 2012;62:677–84.
7. Shvero A, Hubosky SG. Management of upper tract urothelial carcinoma. *Curr Oncol Rep.* 2022;24:611–9.
8. Rouprêt M, Babjuk M, Burger M, Capoun O, Cohen D, Compérat EM, et al. European association of urology guidelines on upper urinary tract urothelial carcinoma: 2020 update. *Eur Urol.* 2021;79:62–79.
9. Lee JY, Kim K, Sung HH, Jeon HG, Jeong BC, Seo SI, et al. Molecular characterization of urothelial carcinoma of the bladder and upper urinary tract. *Transl Oncol.* 2018;11:37–42.
10. Villa E, Ali ES, Sahu U, Ben-Sahra I. Cancer cells tune the signaling pathways to empower de novo synthesis of nucleotides. *Cancers (Basel).* 2019;11:688.
11. Fukada M, Watakabe I, Yuasa-Kawada J, Kawachi H, Kuroiwa A, Matsuda Y, et al. Molecular characterization of CRMP5, a novel member of the collapsin response mediator protein family. *J Biol Chem.* 2000;275:37957–65.
12. Quach TT, Mosinger B, Ricard D, Copeland NG, Gilbert DJ, Jenkins NA, et al. Collapsin response mediator protein-3/unc-33-like protein-4 gene: organization, chromosomal mapping and expression in the developing mouse brain. *Gene.* 2000;242:175–82.
13. Gaetano C, Matsuo T, Thiele CJ. Identification and characterization of a retinoic acid-regulated human homologue of the unc-33-like phosphoprotein gene (hUlip) from neuroblastoma cells. *J Biol Chem.* 1997;272:12195–201.
14. Goshima Y, Nakamura F, Strittmatter P, Strittmatter SM. Collapsin-induced growth cone collapse mediated by an intracellular protein related to UNC-33. *Nature.* 1995;376:509–14.
15. Nagai J, Baba R, Ohshima T. CRMPs function in neurons and glial cells: potential therapeutic targets for neurodegenerative diseases and CNS injury. *Mol Neurobiol.* 2017;54:4243–56.
16. Alabed YZ, Pool M, Tone SO, Sutherland C, Fournier AE. GSK3 beta regulates myelin-dependent axon outgrowth inhibition through CRMP4. *J Neurosci.* 2010;30:5635–43.
17. Alabed YZ, Pool M, Tone SO, Fournier AE. Identification of CRMP4 as a convergent regulator of axon outgrowth inhibition. *J Neurosci.* 2007;27:1702–11.
18. Rosslenbroich V, Dai L, Baader SL, Noegel AA, Gieselmann V, Kappler J. Collapsin response mediator protein-4 regulates F-actin bundling. *Exp Cell Res.* 2005;310:434–44.
19. Kawahara T, Hotta N, Ozawa Y, Kato S, Kano K, Yokoyama Y, et al. Quantitative proteomic profiling identifies DPYSL3 as pancreatic ductal adenocarcinoma-associated molecule that regulates cell adhesion and migration by stabilization of focal adhesion complex. *PLoS ONE.* 2013;8: e79654.
20. Kanda M, Nomoto S, Oya H, Shimizu D, Takami H, Hibino S, et al. Dihydropyrimidinase-like 3 facilitates malignant behavior of gastric cancer. *J Exp Clin Cancer Res.* 2014;33:66.
21. Oya H, Kanda M, Sugimoto H, Shimizu D, Takami H, Hibino S, et al. Dihydropyrimidinase-like 3 is a putative hepatocellular carcinoma tumor suppressor. *J Gastroenterol.* 2015;50:590–600.
22. Chen SL, Cai SR, Zhang XH, Li WF, Zhai ET, Peng JJ, et al. Targeting CRMP-4 by lentivirus-mediated RNA interference inhibits SW480 cell proliferation and colorectal cancer growth. *Exp Ther Med.* 2016;12:2003–8.
23. Li B, Li C. Suppression of prostate cancer metastasis by DPYSL3-targeted saRNA. *Adv Exp Med Biol.* 2017;983:207–16.
24. Tsai YM, Wu KL, Chang YY, Hung JY, Chang WA, Chang CY, et al. Upregulation of Thr/Tyr kinase increases the cancer progression by neurotensin and dihydropyrimidinase-like 3 in lung cancer. *Int J Mol Sci.* 2020;21:1640.
25. Tan F, Wahdan-Alaswad R, Yan S, Thiele CJ, Li Z. Dihydropyrimidinase-like protein 3 expression is negatively regulated by MYCN and associated with clinical outcome in neuroblastoma. *Cancer Sci.* 2013;104:1586–92.
26. Huang WW, Huang HY, Liao AC, Shiue YL, Tai HL, Lin CM, et al. Primary urothelial carcinoma of the upper tract: important clinicopathological factors predicting bladder recurrence after surgical resection. *Pathol Int.* 2009;59:642–9.
27. Yang SH, Li CF, Chu PY, Ko HH, Chen LT, Chen WW, et al. Overexpression of regulator of G protein signaling 11 promotes cell migration and associates with advanced stages and aggressiveness of lung adenocarcinoma. *Oncotarget.* 2016;7:31122–36.
28. Budwit-Novotny DA, McCarty KS, Cox EB, Soper JT, Mutch DG, Creasman WT, et al. Immunohistochemical analyses of estrogen receptor in endometrial adenocarcinoma using a monoclonal antibody. *Cancer Res.* 1986;46:5419–25.
29. McClelland RA, Finlay P, Walker KJ, Nicholson D, Robertson JF, Blamey RW, et al. Automated quantitation of immunocytochemically localized estrogen receptors in human breast cancer. *Cancer Res.* 1990;50:3545–50.
30. Chan TC, Chen YT, Tan KT, Wu CL, Wu WJ, Li WM, et al. Biological significance of MYC and CEBPD coamplification in urothelial carcinoma: multilayered genomic, transcriptional and posttranscriptional positive feedback loops enhance oncogenic glycolysis. *Clin Transl Med.* 2021;11: e674.
31. Pena-Leon V, Perez-Lois R, Seoane LM. mTOR pathway is involved in energy homeostasis regulation as a part of the gut-brain axis. *Int J Mol Sci.* 2020;21:5715.
32. Cancer Genome Atlas Research Network. Comprehensive molecular characterization of urothelial bladder carcinoma. *Nature.* 2014;507:315–22.
33. Massari F, Ciccarese C, Santoni M, Iacovelli R, Mazzucchelli R, Piva F, et al. Metabolic phenotype of bladder cancer. *Cancer Treat Rev.* 2016;45:46–57.
34. Burns JE, Hurst CD, Knowles MA, Phillips RM, Allison SJ. The Warburg effect as a therapeutic target for bladder cancers and intratumoral heterogeneity in associated molecular targets. *Cancer Sci.* 2021;112:3822–34.
35. Hanahan D. Hallmarks of cancer: new dimensions. *Cancer Discov.* 2022;12:31–46.
36. Vander Heiden MG, DeBerardinis RJ. Understanding the intersections between metabolism and cancer biology. *Cell.* 2017;168:657–69.
37. Mercedes SAV, Bocci F, Levine H, Onuchic JN, Jolly MK, Wong PK. Decoding leader cells in collective cancer invasion. *Nat Rev Cancer.* 2016;45:46–57.
38. Lintz M, Muñoz A, Reinhart-King CA. The mechanics of single cell and collective migration of tumor cells. *J Biomech Eng.* 2017;139:0210051–9.
39. Rubtsova SN, Zhitnyak IY, Gloushankova NA. Phenotypic plasticity of cancer cells based on remodeling of the actin cytoskeleton and adhesive structures. *Int J Mol Sci.* 2021;22:1821.
40. Matsunuma R, Chan DW, Kim BJ, Singh P, Han A, Saltzman AB, et al. DPYSL3 modulates mitosis, migration, and epithelial-to-mesenchymal transition in claudin-low breast cancer. *Proc Natl Acad Sci U S A.* 2018;115:E11978–87.
41. Guo H, Xia B. Collapsin response mediator protein 4 isoforms (CRMP4a and CRMP4b) have opposite effects on cell proliferation, migration, and invasion in gastric cancer. *BMC Cancer.* 2016;16:565.
42. Chan TC, Hsing CH, Shiue YL, Huang SK, Hsieh KL, Kuo YH, et al. Angiogenesis driven by the CEBPD-hsa-miR-429-VEGFA signaling axis promotes urothelial carcinoma progression. *Cells.* 2022;11:638.
43. Liberti MV, Locasale JW. The Warburg effect: how does it benefit cancer cells? *Trends Biochem Sci.* 2016;41:211–8.
44. Kang H, Kim H, Lee S, Youn H, Youn B. Role of metabolic reprogramming in epithelial-mesenchymal transition (EMT). *Int J Mol Sci.* 2019;20:2042.
45. Georgakopoulos-Soares I, Chartoumpakis DV, Kyriazopoulou V, Zaravinos A. EMT factors and metabolic pathways in cancer. *Front Oncol.* 2020;10:499.
46. Kim LC, Cook RS, Chen J. mTORC1 and mTORC2 in cancer and the tumor microenvironment. *Oncogene.* 2017;36:2191–201.
47. Lee MN, Ha SH, Kim J, Koh A, Lee CS, Kim JH, et al. Glycolytic flux signals to mTOR through glyceraldehyde-3-phosphate dehydrogenase-mediated regulation of Rheb. *Mol Cell Biol.* 2009;29:3991–4001.
48. Ben-Sahra I, Manning BD. mTORC1 signaling and the metabolic control of cell growth. *Curr Opin Cell Biol.* 2017;45:72–82.

Publisher's Note

Springer Nature remains neutral with regard to jurisdictional claims in published maps and institutional affiliations.